SUPPLEMENTARY FIGURE LEGENDS

Figure S1. The MYST domain of HBO1 can form a stable complex with the N-terminal region of BRPF2 (residues 31-80) with a 1:1 stoichiometry. (A) Schematic illustration of the domain structures of HBO1 and BRPF2. (B) Size-exclusion chromatography of the HBO1 MYST domain and the HBO1 MYST domain in complex with BRPF2(31-80) on a Superdex 200 10/300 column. (C) SDS-PAGE analysis of the HBO1-BRPF2 complex.

Figure S2. Crystal structure of the HBO1-BRPF2 complex. (A, B) Representative simulated annealing composite omit maps of the HBO1-BRPF2 complex. The electron density maps of BRPF2 (A) and AcCoA (B) are contoured at 1.0σ and 1.5σ level, respectively, with the final structure shown in ball-and-stick model. (C) Structure-based sequence alignment of the MYST domains of several representative MYST family HATs. The secondary structures of HBO1 are placed on the top of the alignment. The key residues of the HBO1 MYST domain involved in the interactions with BRPF2 are indicated with dots.

Figure S3. Structural comparisons of the HBO1-BRPF2 complex with other MYST family HATs. (A) Comparison of the MYST domains of HBO1 and MOF (PDB code 2GIV). The zoom-in panel shows a detailed comparison of the key residues at the active site and the AcCoA-binding site of HBO1 and MOF. The key residues and AcCoA are represented with ball-and-stick models. (B) Comparison of the HBO1-BRPF2 complex and the MOF-MSL1 complex (PDB code 2Y0M).

Figure S4. Sequence alignments of the scaffold proteins. (A) Sequence alignments

of the BRPF family members and BRPF2 from different species. The key residues involved in the hydrophobic interactions with HBO1 are indicated with spheres, and the acidic residues forming the two negatively charged surface patches with triangles. (B) Sequence alignment of the BRPF, JADE and EPC family proteins. Domain I of JADE1 is the region interacting with the MYST domain of HBO1.

Figure S5. A structure model showing the relationship between the potential histone-binding site of BRPF2 and the substrate-binding site of HBO1. The structure model is built based on the superposition of the HBO1-BRPF2 complex with the Gcn5-H3(9-19) peptide complex (PDB code 1QSN). The H3 peptide is colored in red. The two acidic patches of BRPF2 are shown with side chains. The distance between the C-terminal of the H3 peptide and the acidic patches of BRPF2 are indicated with dotted lines.

Figure S6. A working model for the potentiation of the HAT activity of HBO1 by BRPF2. The N-terminal region of BRPF2 can interact with HBO1 to stabilize its conformation, and additionally it can also interact with the N-terminal tail of H3 although BRPF2 binds to nucleosomes mainly via the PZP, bromo and PWWP domains. The concurrent binding of BRPF2 with both HBO1 and histone H3 can properly position the N-terminal tail of H3 at the active site of HBO1 for acetylation and thus enhance the HAT activity of the HBO1 HAT complex. It is also possible that the binding of the N-terminal region of BRPF2 can stabilize HBO1 in a more physiological conformation and hence enhances its interaction with histone substrate, leading to the potentiation of the HAT activity of HBO1.

Figure S1

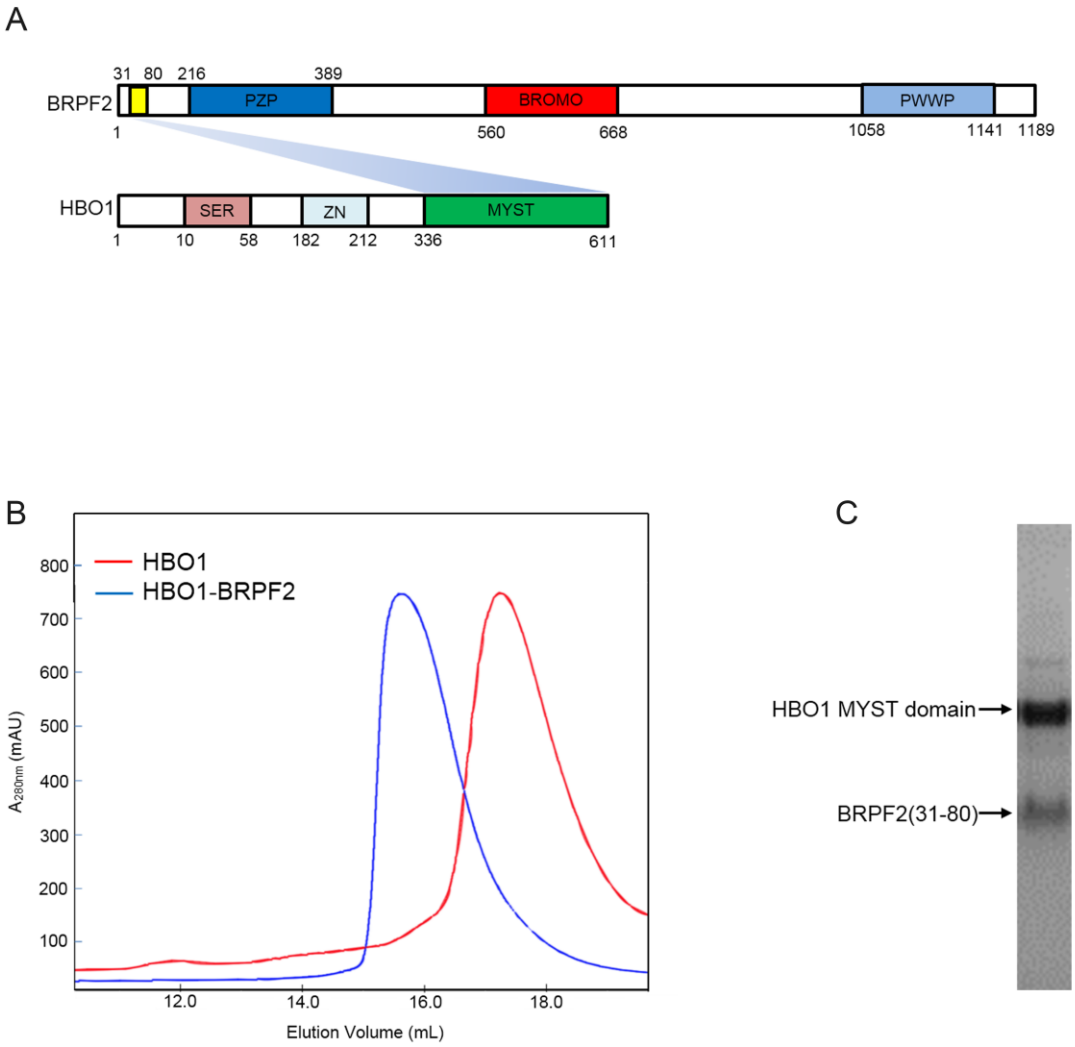
A
31 80 216 389
BRPF2
PZP
BROMO
PWWP
1 560 668 1058 1141 1189
HBO1
SER
ZN
MYST
1 10 58 182 212 336 611
B
HBO1
HBO1-BRPF2
800
700
600
500
400
300
200
100
A280nm (mAU)
12.0
14.0
16.0
18.0
Elution Volume (mL)
C
HBO1 MYST domain
BRPF2(31-80)

Figure S2

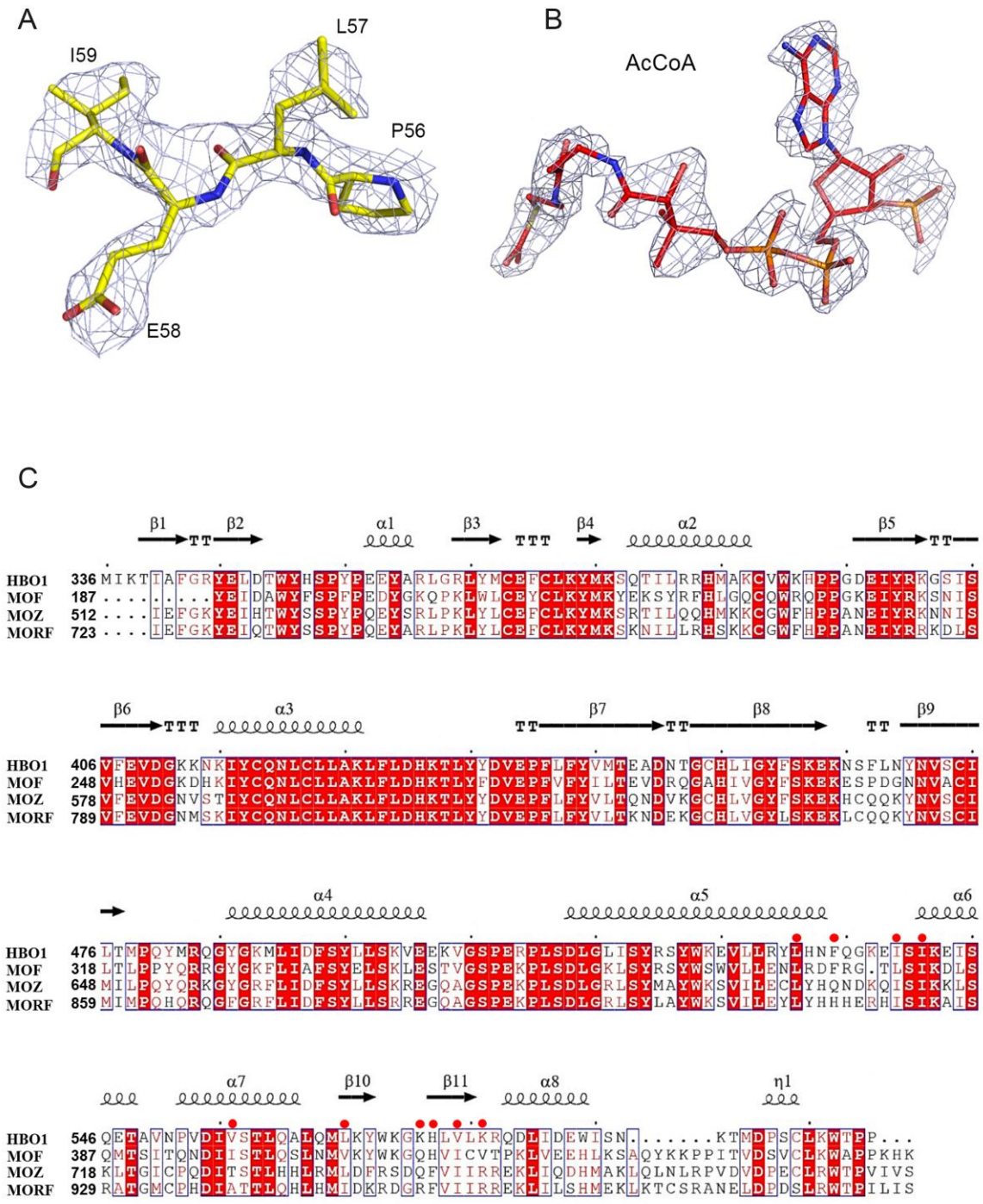
A
L57
I59
P56
E58
B
AcCoA
C
HBO1 336 MIKTIAFGRYELDTWYHSPYPEEYARLGRLYMCEFCLKYMKSQTILRRHMAKCVWKHPPGDEIYRKGSIS
MOF 187 ....YEIDAWYFSPFPEDYGKQPKLWLCEYCLKYMKYEKSYRFHLGQCQWRQPPGKEIYRKSNIS
MOZ 512 ....IEFGKYEIHTWYSSPYPQEYSRLPKLYLCEFCLKYMKSRTILQQHMKKCGWFHPPANEIYRKNNIS
MORF 723 ....IEFGKYEIQTWYSSPYPQEYARLPKLYLCEFCLKYMKSKNILLRHSKKCGWFHPPANEIYRRKDLS
HBO1 406 VFEVDGKKNKIYCQNLCLLAKLFLDHKTLYYDVEPFLFYVMTEADNTGCHLIGYFSKEKNSFLNYNVSCI
MOF 248 VHEVDGKDHKIYCQNLCLLAKLFLDHKTLYFDVEPFVFYILTEVDRQGAHIVGYFSKEKESPDGNNVACI
MOZ 578 VFEVDGNVSTIYCQNLCLLAKLFLDHKTLYYDVEPFLFYVLTQNDVKGCHLVGYFSKEKHCQQKYNVSCI
MORF 789 VFEVDGNMSKIYCQNLCLLAKLFLDHKTLYYDVEPFLFYVLTKNDEKGCHLVGYLSKEKLCQQKYNVSCI
HBO1 476 LTMPQYMRQGYGKMLIDFSYLLSKVEEKVGSPERPLSDLGLISYRSYWKEVLLRYLHNFQGKEISIKEIS
MOF 318 LTLPPYQRRGYGKFLIAFSYELSKLESTVGSPEKPLSDLGKLSYRSYWSWVLLENLRDFRG.TLSIKDLS
MOZ 648 MILPQYQRKGYGRFLIDFSYLLSKREGQAGSPEKPLSDLGRLSYMAYWKSVILECLYHQNDKQISIKKLS
MORF 859 MIMPQHQRQGFGRFLIDFSYLLSRREGQAGSPEKPLSDLGRLSYLAYWKSVILEYLYHHHERHISIKAIS
HBO1 546 QETAVNPVDIVSTLQALQMLKYWKGKHLVLKRQDLIDEWISN.....KTMDPSCLKWTPP...
MOF 387 QMTSITQNDIISTLQSLNMVKYWKGQHVICVTPKLVEEHLKSAQYKKPPITVDSVCLKWAPPKHK
MOZ 718 KLTGICPQDITSTLHHLRMLDFRSDQFVIIRREKLIQDHMAKLQLNLRPVDVDPECLRWTPVIVS
MORF 929 RATGMCPHDIATTLQHLHMIDKRDGRFVIIRREKLILSHMEKLKTCSRANELDPDSLRWTPILIS

Figure S3

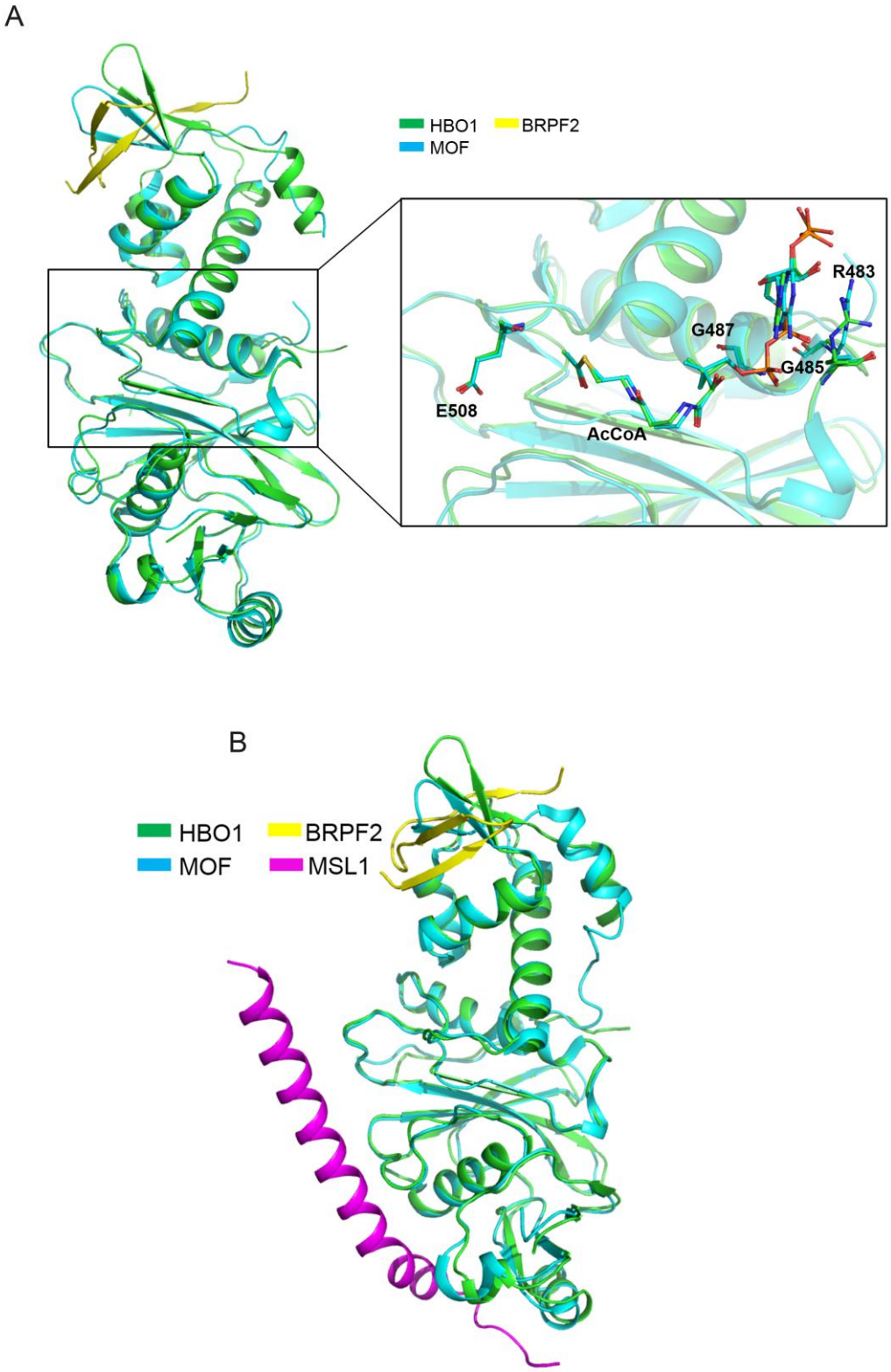
A
HBO1
BRPF2
MOF
R483
G487
G485
E508
AcCoA
B
HBO1
BRPF2
MOF
MSL1

Figure S4

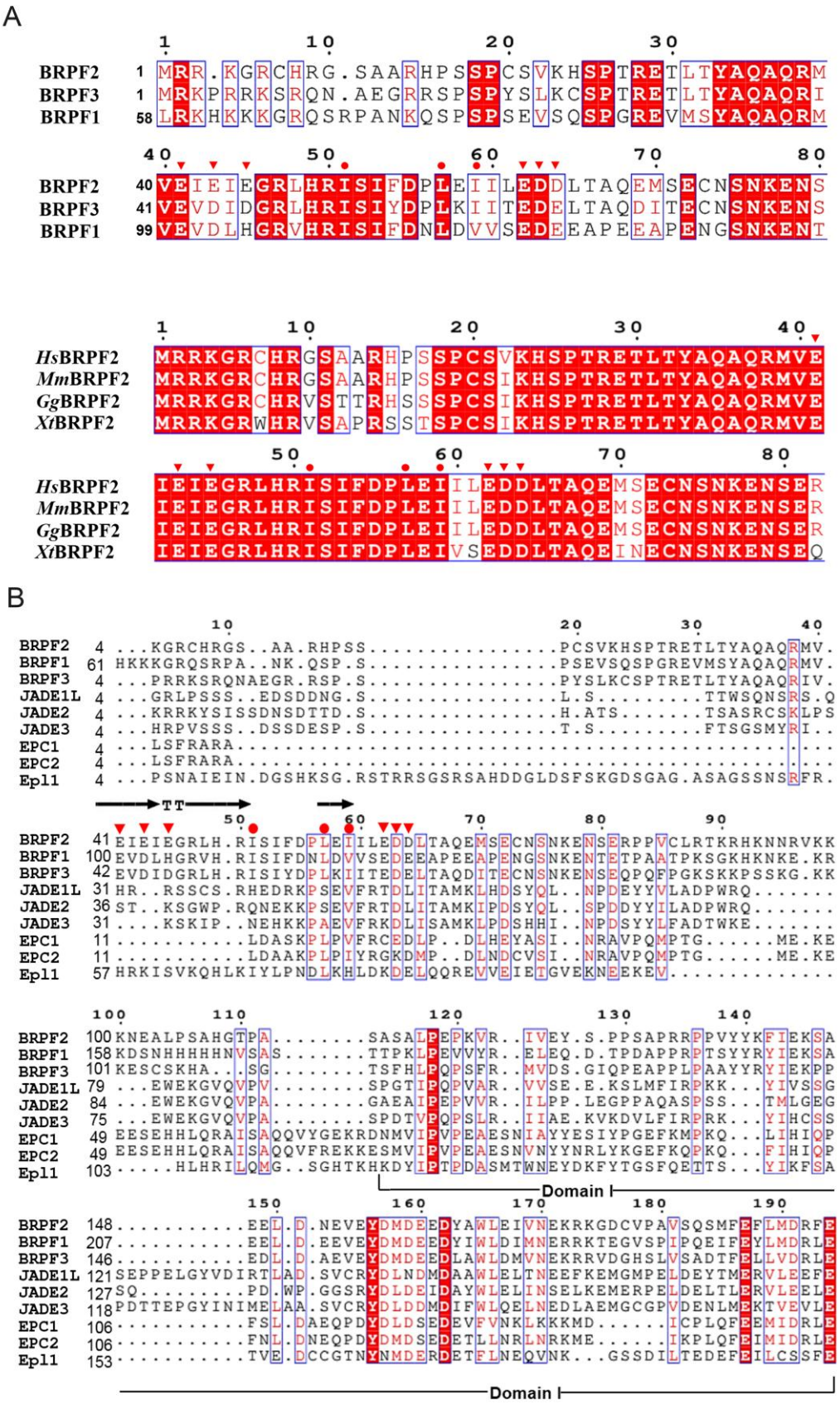
A
BRPF2
BRPF3
BRPF1
HsBRPF2
MmBRPF2
GgBRPF2
XtBRPF2
B
BRPF2
BRPF1
BRPF3
JADE1L
JADE2
JADE3
EPC1
EPC2
Epl1
Domain
Domain

Figure S5

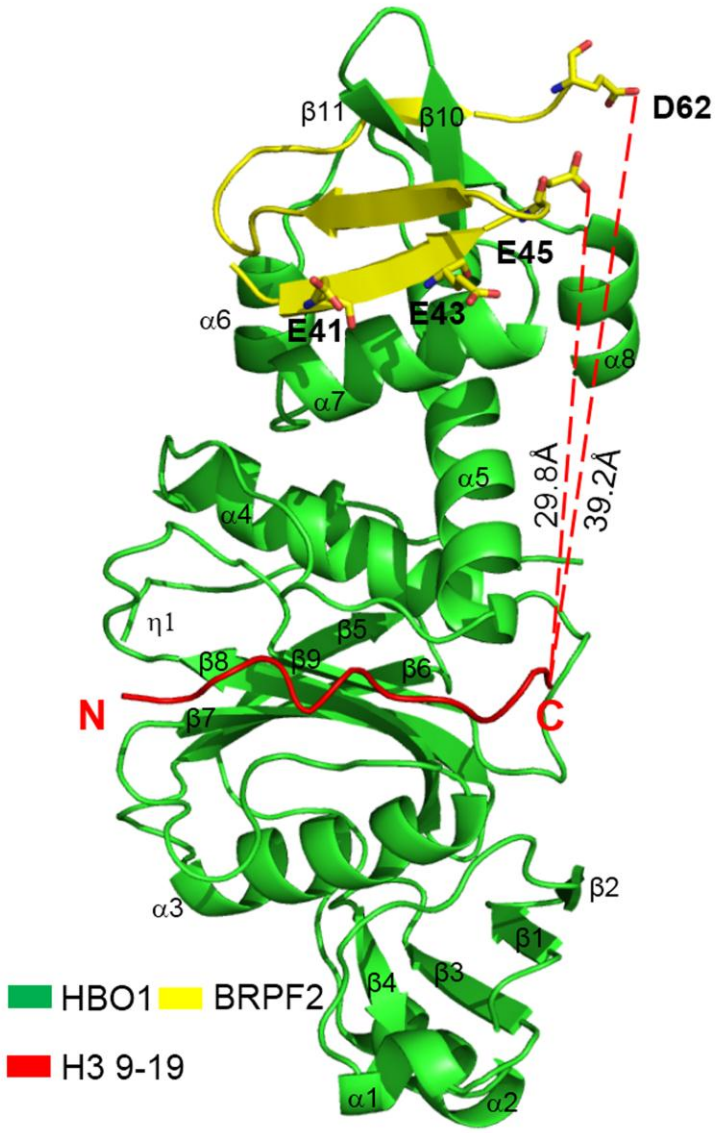
β11
β10
D62
E45
E43
E41
α6
α8
α7
α5
α4
29.8Å
39.2Å
η1
β5
β8
β9
β6
N
β7
C
α3
β2
β1
β3
β4
HBO1
BRPF2
H3 9-19
α1
α2

Figure S6